

# Electro Analytical Studies on the Interaction and Corrosion Inhibition of a Triazine Dimer (AMTDT) on Metallic Copper in Hydrochloric Acid

Shainy K.M. and Abraham Joseph\*

Department of Chemistry, University of Calicut, Calicut University P O, Kerala, India.  
(\*E-mail drabrahamj@gmail.com)

**Abstract:** The effect of corrosion inhibition of a triazine dimer (E)-4-((4-amino-6-methyl-3-thioxo-3,4-dihydro-1,2,4-triazin-5(2H)-ylidene)amino)-6-methyl-3-thioxo-3,4-dihydro-1,2,4-triazin-5(2H)-one.bis[4-amino-3-mercapto-6-methyl-1,2,4-triazin-2(H)-5(one)] (AMTDT) on copper in 0.5M, 1M and 2M HCl at different temperatures has been investigated by polarization, EIS, adsorption, surface studies, and computational calculations. The results of electrochemical impedance and Tafelpolarization measurements show that AMTDT acts as a good corrosion inhibitor. The inhibition efficiency increases with increasing concentration of AMTDT and decreases with acid concentration and temperature. AMTDT was more efficient at 313K compared to 303K and 323K. The mechanism involves adsorption and the process follows Langmuir isotherm and the adsorption process is temperature dependent. The theoretical parameters were also calculated using density functional theory at the level of B3LYP/6-31G\* and found to be in support of the experimental result.

**Key Words:** Copper, Schiff base, acid solution, adsorption, polarization, EIS.

## INTRODUCTION

Selection of an effective corrosion inhibitor is very important to protect metals and metal based objects, when it is exposed to acidic or alkaline environment. Copper is a noble metal with valuable properties such as high electrical conductivity and thermal conductivity, but it undergoes corrosion in acidic and strong alkaline media. Most of the time tested inhibitors are aromatic compounds containing N, S, O, and P atoms or systems with conjugated pi electron network. The heterocyclic compounds which contain N, S, and O atoms can also form chelates with metal and form a film on the surface, which in turn prevents the attack of H<sup>+</sup> ions, and resists corrosion [1-8]. Schiff base is another class of compounds which can act as inhibitors due to the presence of electron rich groups like >C=N- and their inhibiting efficiency is more encouraging than corresponding aldehydes and amines [9-10].

The blocking of metal surface from the corrosive medium is mainly by the adsorption of inhibitor molecules on the metal surface. The adsorption ability of metals depends on the nature and surface charge of the metal, chemical composition of electrolytes, molecular structure, and electronic characteristic of inhibitor. The process of adsorption may be of different types, (1) electrostatic attraction between charged molecules and charged metal, (2) interaction of unshared electron pairs in the molecules with metal, (3) interaction of π electron with metal, and/or (4) combination of all these processes [11-12].

Recently, some triazine molecules and their derivatives were reported to act as good corrosion inhibitors for mild steel and copper. The choice of these compounds was based on the inherent properties they possess like π-electron conjugation, abundance of heteroatom, ability of coordination, and adsorption on to copper metal [13-15].

The present study aims to investigate the effect of inhibitor, (E)-4-((4-amino-6-methyl-3-thioxo-3,4-dihydro-1,2,4-triazin-5(2H)-ylidene)amino)-6-methyl-3-thioxo-3,4-dihydro-1,2,4-triazin-5(2H)-one, a triazine dimer on copper corrosion in 0.5M, 1M and 2M HCl solutions, using electrochemical techniques such as electrochemical impedance spectroscopy and Tafel polarization. The mechanism of inhibition was ascertained by scanning electron microscopy and adsorption studies. In order to investigate the relationship between the inhibitor efficiency and structure of the molecule, some quantum chemical parameters such as HOMO and LUMO energies, charge density on adsorption center, and dipole moment etc have been calculated.

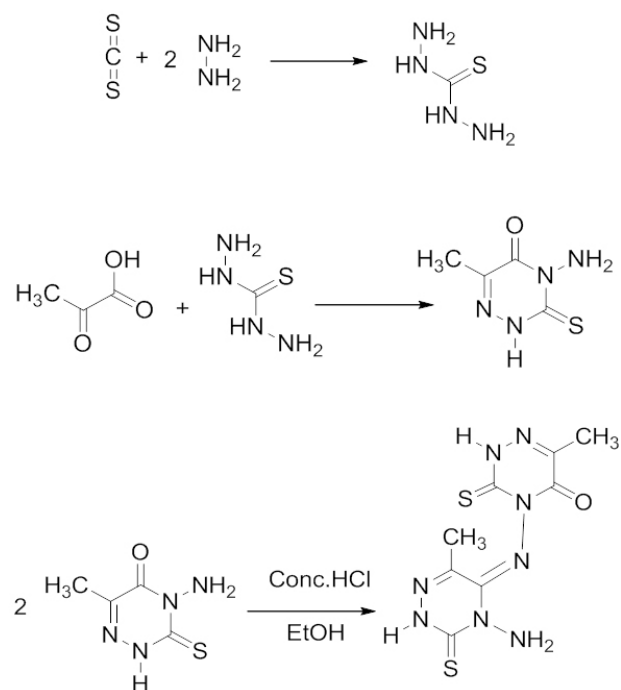
## EXPERIMENTAL METHODS

### Synthesis of Inhibitor Molecule AMTDT

The inhibitor molecule, AMTDT, was synthesized by a three stage reaction. In the first stage, carbon disulfide (E. Merck Germany) reacted with hydrazine mono hydrate (E. Merck) to form thiocarbohydrazide. The thiocarbohydrazide reacted with 2-oxopropionic acid (E. Merck) which led to the formation of [4- amino 3-mercapto 6-methyl -1, 2, 4-triazin 2(H)- 5one] in the second stage [16-17]. At the final stage, [ 4- amino 3-mercapto 6-methyl -1,2,4-triazin 2(H)- 5one] dimerized to form (E)-4-((4-amino-6-methyl-3-thioxo-3,4-dihydro-1,2,4-triazin-5(2H)-ylidene)amino)-6-methyl-3-thioxo-3,4-dihydro-1,2,4-triazin-5(2H)-one in the presence of conc. HCl and ethanol under reflux for 4 hours. The product was re-crystallized from alcohol and characterized by spectral and elemental analysis. The compound was soluble in HCl and was used for the investigation. Synthesis of AMTDT is shown in Scheme 1.

### Material and Medium

The copper specimens of dimensions 2.8x1.9cm<sup>2</sup> were selected and polished with different grade emery papers followed by washing with water and acetone and were used in electrochemical measurements. The test solution was prepared from reagent grade HCl (E. Merck) and distilled water [18]. All the tests were performed in aerated medium at room temperature (303K) and high temperatures (313K and 323K).



**Scheme 1. Synthesis of AMTDT**

### Electrochemical Measurements

The electrochemical measurements were carried out by a computer controlled electrochemical work station (ACM, UK model no.1745). It consisted of a three electrode corrosion cell with platinum foil (1 cm<sup>2</sup> surface area), used as the auxiliary electrode, and saturated calomel electrode (SCE) as the reference electrode. The working electrode was a copper metal piece, which was immersed in the test solution firstly. Prior to the electrochemical measurements, a stabilization period of 60 minutes was allowed to attain a stable value of  $E_{\text{corr}}$  [19].

The electrochemical impedance measurements were carried out in a frequency range of 0.01 to 1000 Hz, with amplitude of 5mV. The impedance diagrams were plotted in the Nyquist representation. The double layer capacitance ( $C_{\text{dl}}$ ) calculated [20] from the equation:

$$C_{\text{dl}} = \frac{1}{2\pi f_{\text{max}} R_{\text{ct}}} \quad (1)$$

where  $f_{\text{max}}$  is the frequency at which the imaginary component of impedance is maximum.

The percentage inhibition efficiency (IE %) was calculated from charge transfer resistance by the equation:

$$\text{IE (\%)} = \frac{R_{\text{ct}}^* - R_{\text{ct}}}{R_{\text{ct}}^*} \times 100 \quad (2)$$

where  $R'_{ct}$  and  $R_{ct}$  are the charge-transfer resistance in the presence and absence of inhibitor AMTDT.

The potentiodynamic polarization was carried out from the cathodic potential -250mV versus  $E_{corr}$  to anodic potential of +250mV versus  $E_{corr}$ , with a scan rate 1mV/s. The linear Tafel segments of the cathodic and anodic curves were extrapolated to corrosion potential, to obtain the corrosion current densities, which were used to calculate inhibition efficiency.

The percentage inhibition efficiency was calculated from the equation of polarization measurements:

$$IE \% = \frac{I_{Corr}^* - I_{Corr}}{I_{Corr}^*} \times 100 \quad (3)$$

where  $I_{corr}^*$  and  $I_{corr}$  are the corrosion current densities of the inhibited and uninhibited copper metal.

### Surface Characterization

The scanning electron microscopy measurements of the metal specimens were done in Hitachi SU 6600, instrument at an accelerating voltage 20.0Kv and at a 500X magnification. The metal specimens were immersed in acid solution containing optimum concentration of inhibitor for 4 hours, and then removed, rinsed with acetone and dried, and used for measurements.

### Computational Studies

The quantum chemical calculations were performed with complete geometry optimization of the inhibitor molecule using density functional theory at B3LYP/6-31G\* level and the frequency calculation was also done with the same level of DFT to get energy minima using Gaussian 03 software package. The energies of the frontier molecular orbital (HOMO and LUMO) can be used to calculate and interpret the adsorption characteristics of the inhibitor molecule.

According to Koopman's theorem, the following theoretical relations can be arrived between the chemical potential of molecule, such as ionization potential, electron affinity, electronegativity, hardness, softness, and corresponding Frontier molecular orbitals, and have been well established in conceptual density functional theory [21].

$$I = -E_{HOMO} \quad (4)$$

$$A = -E_{LUMO} \quad (5)$$

$$X = -\mu = \frac{I+A}{2} \quad (6)$$

$$\eta = \frac{I+A}{2} \quad (7)$$

$$\sigma = \frac{1}{\eta} \quad (8)$$

The fraction of electro transferred from the inhibitor to the metal surface can be predicted as:

$$\Delta N = \frac{\chi_m - \chi_{inh}}{2(\eta_m - \eta_{inh})} \quad (9)$$

where  $\chi_m$  and  $\chi_{inh}$  represents the electro negativity of Fe and inhibitor molecule and  $\eta_m$  and  $\eta_{inh}$  are the hardness of the metal and inhibitor, respectively. Theoretically, we assume that the value of  $\chi_{Fe}$  is 7.0eV and  $\eta_{Fe}$  is zero.

## RESULTS & DISCUSSION

### Characterization of (E)-4-((4-amino-6-methyl-3-thioxo-3,4-dihydro-1, 2, 4-triazin-5(2H)-ylidene) amino)-6-methyl-3-thioxo-3, 4-dihydro-1, 2, 4-triazin-5(2H)-one

The synthesized inhibitor AMTDT was characterized by elemental analysis, FTIR, <sup>1</sup>H NMR, and Mass spectra. CHNS (%) found (calculated) C: 32.34 (32.21), H: 2.63 (3.38), N: 37.62 (37.58), S: 19.11 (21.47). FTIR (KBr);  $\nu = 1662\text{cm}^{-1}$  (C=N- stretch), 1235 and 891 $\text{cm}^{-1}$  (C=S stretch), 1128  $\text{cm}^{-1}$  (N-N stretch), 2907 $\text{cm}^{-1}$  (C-H stretch), 3216  $\text{cm}^{-1}$  (N-H stretch). The <sup>1</sup>HNMR spectrum of AMTDT in dms<sub>o</sub>-d<sub>6</sub>, (Fig.1) shows the chemical shifts ( $\delta$ /ppm) at  $\delta = 6.45$ ppm assignable to secondary N-H proton. A singlet of three protons at  $\delta = 2.17$ ppm was assignable to methyl protons.

Mass spectrum of AMTDT was recorded HRMS-FAB method and is represented in Fig.2. It shows the molecular ion peak at m/z 298.68 (41%) with a base peak at m/z 215.21 (100.00 %). This is in addition to the other significant peaks at m/z 197.25 (60 %), 280.23 (67 %), 109 (63%), 179.24 (30 %), 149.23 (39 %).

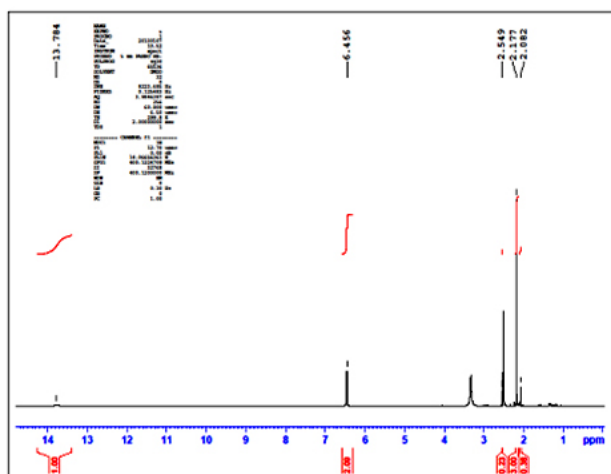


Fig 1. <sup>1</sup>H NMR Spectra of AMTDT

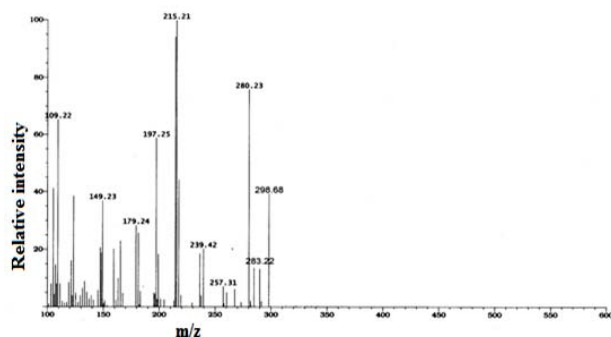


Fig 2. MASS Spectra of AMTDT

## Electrochemical Impedance Spectroscopy (EIS)

The impedance measurements were carried out after an immersion time of one hour in 0.5M, 1M and 2M HCl solutions at 303K, 313K, and 323K in the presence and absence of different concentrations of AMTDT. The results were recorded as Nyquist plots. It contains semicircles whose size increases with increasing inhibitor concentration and a representation corresponding to 303K is given in Fig.3. The corresponding electrochemical parameters, namely the charge transfer resistance ( $R_{ct}$ ), double layer capacitance ( $C_{dl}$ ), corrosion rate (CR mils/year), and percentage inhibition efficiency were calculated. Among these the  $R_{ct}$ , CR (mils/year), and percentage inhibition efficiency were listed in Tables 1, 2, and 3. The values of  $R_{ct}$  and  $C_{dl}$  exhibit opposite trends over the entire concentration range. The  $R_{ct}$  values increased with increasing inhibitor concentration, which indicates considerable surface coverage by the inhibitor and a bonding between the surface of the metal to the inhibitor [22]. The decrease in  $C_{dl}$  value suggests that strong adsorption of the inhibitor on the surface of copper, which revealed that an increase in the thickness of the protective layer. The mechanism of adsorption involves blocking of reaction sites on the surface by adsorbing the inhibitor [23-26], which increases with concentration of inhibitor and decreases with temperature. But at higher temperature 323K, the  $C_{dl}$  values indicate that there is a weak adsorption on the metal.

Table 1. Electrochemical data for copper corrosion in different concentrations of HCl in the presence and absence of inhibitor AMTDT at 303K

Acid conc.(M)	Inhibitor conc.(ppm)	EIS Parameters			Polarization Parameters		
		$R_{ct}$	CR (mils/yr)	%IE	$I_{corr}$	CR (mils/yr)	%IE
0.5	Blank	349.9	68.31	---	0.0239	21.89	---
	50	815.8	29.28	57	0.0039	3.54	83
	100	1245	19.19	71	0.0037	3.45	84
	150	1758	13.59	80	0.0024	2.24	89
	200	2517	9.49	86	0.0018	1.71	92
1	Blank	494.5	48.37	---	0.0225	20.61	---
	50	1050	22.21	52	0.0095	8.78	57
	100	1396	17.11	64	0.0071	6.55	68
	150	1641	14.56	69	0.0069	5.82	71
	200	1790	13.35	72	0.0062	5.74	72
2	Blank	501.1	47.13	---	0.0203	18.60	---
	50	942.4	25.35	46	0.0090	8.25	55
	100	1194	20.01	58	0.0079	7.28	61
	150	1275	18.74	60	0.0074	6.79	63
	200	1362	17.54	63	0.0065	6.01	68

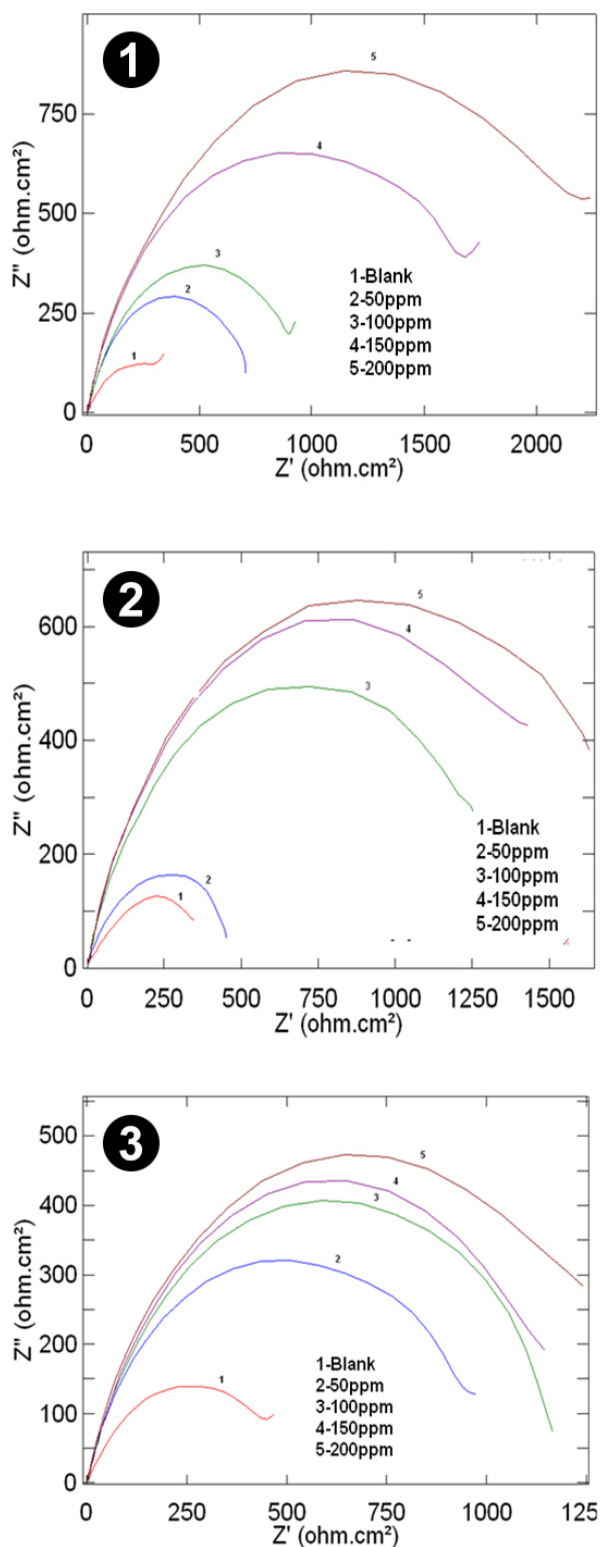


**Fig 3. Nyquist plots for copper corrosion in (1) 0.5M, (2) 1M, (3) 2M HCl in the absence and presence of different concentrations of AMTDT at 303K**

### Tafel Polarization

The potentiodynamic polarization curves for copper in 0.5M, 1M, and 2M HCl solutions at 303K, 313K and 323K in the presence and absence of inhibitor AMTDT were recorded, and presentation corresponding to 303K shown in Fig.4. The electrochemical parameters, such as corrosion potential ( $E_{\text{corr}}$ ), corrosion current density ( $I_{\text{corr}}$ ) cathodic and anodic Tafel slopes ( $\beta_a$  and  $\beta_c$ ), were obtained from the Tafel polarization plots, in which  $I_{\text{corr}}$  and CR (mils/year) were listed in Tables 1, 2, and 3.

The inhibition efficiency of AMTDT increases with increasing concentration, which is the major result of polarization study and is parallel to the EIS result. In the acidic solution, cathodic reaction is the discharge of  $\text{H}^+$  ions to hydrogen gas or reduced oxygen and the anodic reaction involves the passage of metal ion from the metal solution. Generally, an inhibitor might affect either anodic or cathodic reactions or both in some cases. But in this case, the inhibitor AMTDT effect anodic and cathodic curves of polarization and shifted both to lower current densities and AMTDT act as a mixed type inhibitor [27].

The investigation of the effect of temperature on the inhibitor has led to an important observation. The solubility of the inhibitor is low at room temperature. Therefore, at higher temperature (313K) a more effective protective layer is formed on the surface of the metal. This explains the increased efficiency of the inhibitor at 313K. But when the temperature was further increased to 323K, the efficiency was found to decrease. The adsorption of inhibitor molecules on the metal surface can be considered as a combination of physisorption and chemisorptions, with physisorption as the major contributor. The effect of physisorption decreases with increasing temperature. Therefore, as the temperature was increased, efficiency of adsorption of inhibitor molecules on to the metal surface would decrease. This explains the low inhibition efficiency of the inhibitor at 323K [28]. Thus, 313K is the optimum temperature for the inhibitor AMTDT.

**Table 2. Electrochemical data for copper corrosion in different concentrations of HCl in the presence and absence of inhibitor AMTDT at 313K**

Acid conc.(M)	Inhibitor conc.(ppm)	EIS Parameters			Polarization Parameters		
		R <sub>ct</sub>	CR (mils/yr)	%IE	I <sub>corr</sub>	CR (mils/yr)	%IE
0.5	Blank	73.21	157.2	----	0.0208	19.07	----
	50	311.1	76.79	40	0.0055	5.06	73
	100	459.2	52.2	76	0.0040	3.75	81
	150	589.7	40.51	87	0.0026	2.4	87
	200	1234	19.36	94	0.0016	1.51	94
1	Blank	109.9	217.4	----	0.0901	82.58	----
	50	269.2	88.74	59	0.0035	32.49	60
	100	797.5	29.95	86	0.0092	8.47	89
	150	1020	23.42	89	0.0070	6.47	92
	200	1840	12.98	94	0.0051	4.32	94
2	Blank	102.2	233.7	----	0.0228	20.96	----
	50	614.1	38.90	83	0.0041	3.84	81
	100	1349	17.20	90	0.0020	1.85	91
	150	1517	15.54	92	0.0016	1.52	93
	200	2820	8.38	93	0.0012	1.15	94

**Table 3. Electrochemical data for copper corrosion in different concentrations of HCl in the presence and absence of inhibitor AMTDT at 323K**

Acid conc.(M)	Inhibitor conc.(ppm)	EIS Parameters			Polarization Parameters		
		R <sub>ct</sub>	CR (mils/yr)	%IE	I <sub>corr</sub>	CR (mils/yr)	%IE
0.5	Blank	301.3	79.29	----	0.0399	36.54	----
	50	910.7	26.23	66	0.0994	8.65	76
	100	998.5	23.92	69	0.0790	7.24	80
	150	1278	18.67	76	0.0670	6.2	83
	200	5275	4.52	94	0.0021	2.00	94
1	Blank	213.2	121.1	----	0.0185	17.01	----
	50	348.2	96.64	39	0.0096	8.86	47
	100	1171	20.40	79	0.0050	4.64	73
	150	1721	13.88	86	0.0031	2.88	83
	200	1983	11.27	89	0.0018	1.65	90
2	Blank	358.9	66.56	----	0.0121	11.09	----
	50	668.8	35.72	46	0.0058	5.38	52
	100	754.9	31.16	52	0.0042	3.86	65
	150	1154	20.70	68	0.0030	2.81	75
	200	1882	10.95	84	0.0021	1.97	82

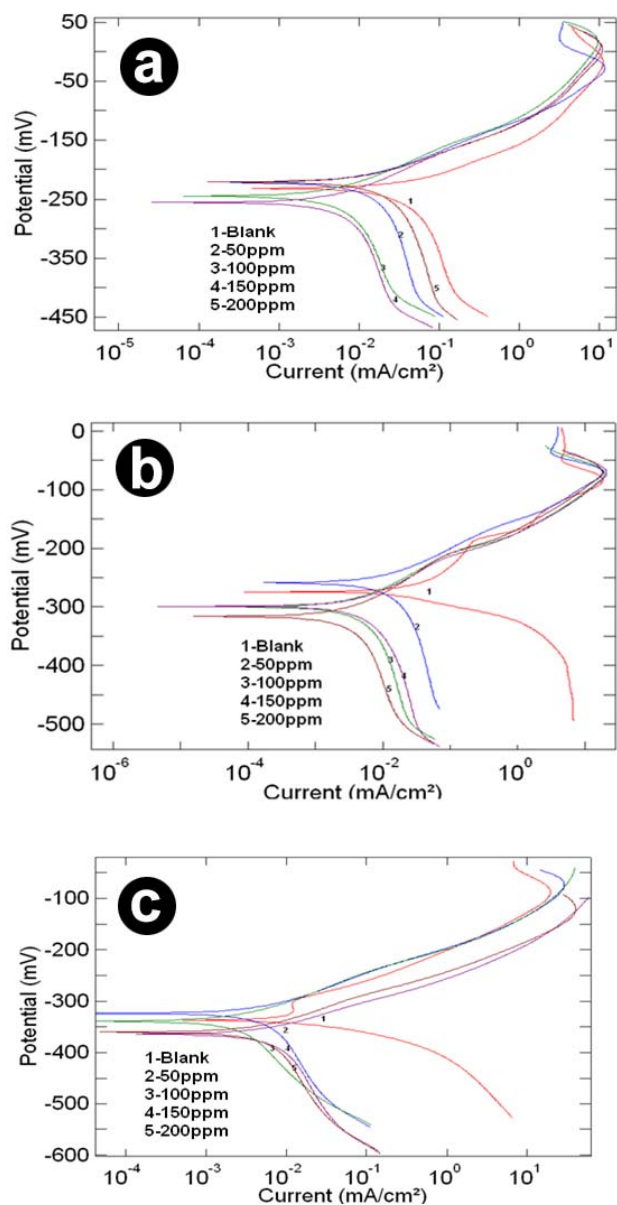


**Fig 4. Tafel polarization curves for copper corrosion in (a) 0.5M, (b) 1M, (c) 2M HCl in the absence and presence of different concentrations of AMTDT at 303K.**

#### Adsorption Studies

The metal surface adsorbs the inhibitor, thus it can accelerate the reaction kinetics either by adsorbing the available surface area for corrosion or by modifying the electrochemical standard Gibbs free energy of activation [29]. Surface coverage  $\theta$ , for different concentration of inhibitor 0.5M, 1M, and 2M HCl solutions at 303K, 313K, and 323K have been obtained from potentiodynamic

polarization measurements. The relationship of  $C/\theta$  (ppm) versus  $C_{inh}$  (ppm) in Fig. 5 suggests that the adsorption of AMTDT on copper followed the Langmuir adsorption isotherm, which is the best fit. The isotherm can be represented as:

$$\frac{C_{inh}}{\theta} = C_{inh} + \frac{1}{K_{ads}} \quad (10)$$

where  $C_{inh}$  is the concentration of inhibitor in mol/L and  $K_{ads}$  is the equilibrium constant of adsorption.

The standard Gibbs free energy of adsorption  $\Delta G^0_{ads}$  and adsorption constant ( $K_{ads}$ ) related by the equation:

$$\Delta G^0_{ads} = -RT \ln(55.5 K_{ads}) \quad (11)$$

The negative values of  $\Delta G^0_{ads}$  indicate the stability of the adsorbed layer on the copper surface and spontaneity of the process [30]. The perusal of  $\Delta G^0_{ads}$  ranges from -29 to -38KJ/mol, which suggest that the adsorption of AMTDT follows two types of interactions: physisorption and chemisorptions [31].

#### Computational Studies

In the AMTDT, all the experimental results were in good agreement with theoretically predicted results generated at the B3LYP/6-31G\* level of DFT.

The inhibition efficiency of an inhibitor depends on the molecular structure of that inhibitor [32]. The degree of corrosion inhibition was correlated with energy of highest occupied molecular orbital ( $E_{HOMO}$ ), lowest unoccupied molecular orbital ( $E_{LUMO}$ ), energy gap ( $\Delta E = E_{LUMO} - E_{HOMO}$ ), the dipole moment ( $\mu$ ), and ionization potential (I).

The ionization potential of a molecule, which is closely related to  $E_{HOMO}$ , higher value of  $E_{HOMO}$  (-6.0873 eV), indicates the tendency of AMTDT to donate an electron to the acceptor copper surface, and facilitate the adsorption and therefore, enhance the inhibition efficiency. Similarly, the lower value of  $E_{LUMO}$  (-2.1832 eV) indicates the ability to accept an electron from AMTDT and hence, possible better inhibition efficiency [33]. The theoretical models for explaining structure and conformation barrier in the molecular system can be obtained by the energy gap of the inhibitor ( $\Delta E = E_{LUMO} - E_{HOMO}$ ). The lower gap of LUMO-HOMO of AMTDT also

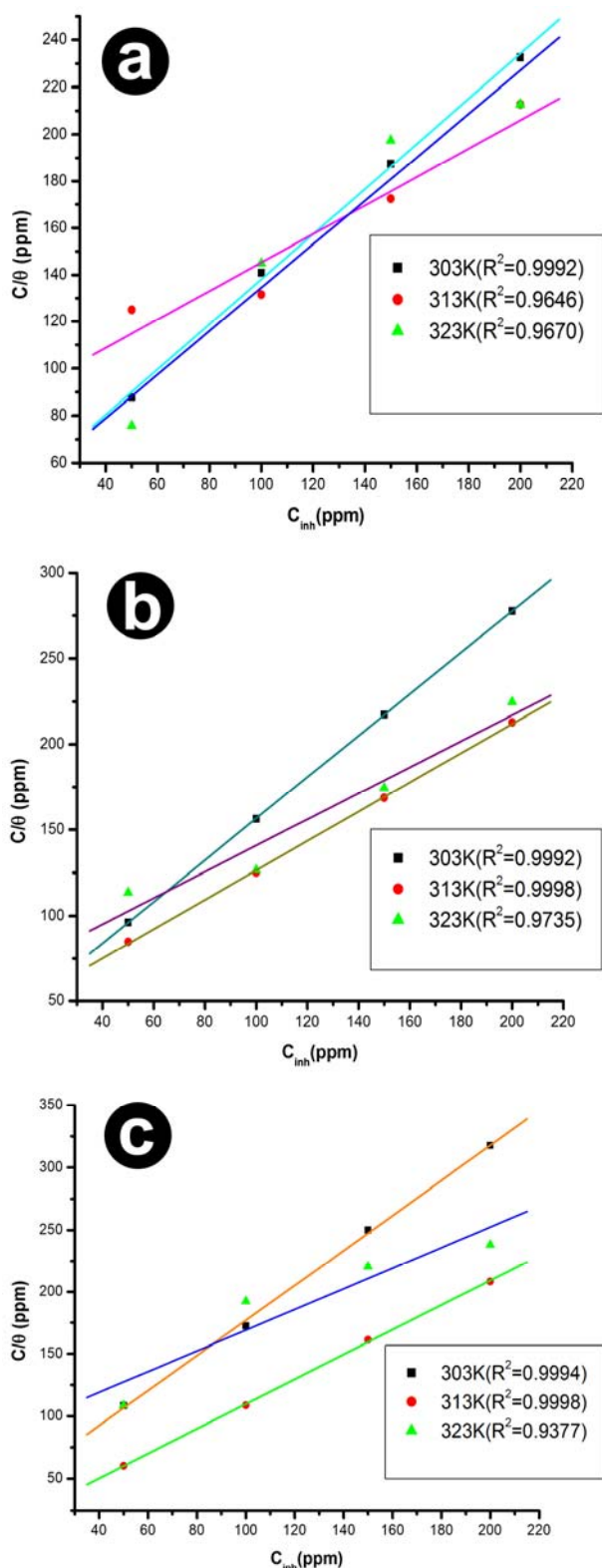


**Fig 5. Langmuir adsorption plots for copper in (a) 0.5M, (b) 1M (c) 2M HCl in AMTDT inhibitor at 303, 303 and 323K temperature**

supports the better inhibition efficiency [34]. The lower value of chemical softness (0.5123) confirms higher reactivity of AMTDT [35-36].

The dipole moment of AMTDT (1.3883 D) indicating polarity reveals the ability to donate electrons to the metal surface. The fraction of electron transferred from the AMTDT to the mild steel surface showing the higher inhibition efficiency of AMTDT. The theoretical parameters and chemical reactivity descriptors such as ionization potential, electronegativity, hardness, and softness are demonstrated in Table 4. The optimized geometry, HOMO, LUMO of AMTDT are given in Figure 6.

**Table 4. Calculated quantum chemical parameters for the Inhibitor AMTDT**

Quantum chemical parameters of AMTDT	
$E_{total}$ (eV)	-44092.3
$E_{HOMO}$ (eV)	-6.0873
$E_{LUMO}$ (eV)	-2.1832
$\Delta E$ (eV)	3.9041
$I$ (eV)	6.0873
$A$ (eV)	2.1832
$\chi$ (eV)	4.1352
$\eta$ (eV)	1.9520
$\mu$ (D)	1.3883
$\sigma$	0.5123
$\Delta N$	0.7338

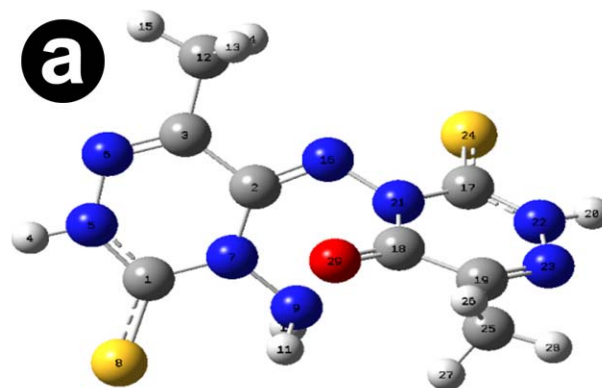


**Fig 6. (a) Optimized molecular structure of the inhibitor AMTDT**

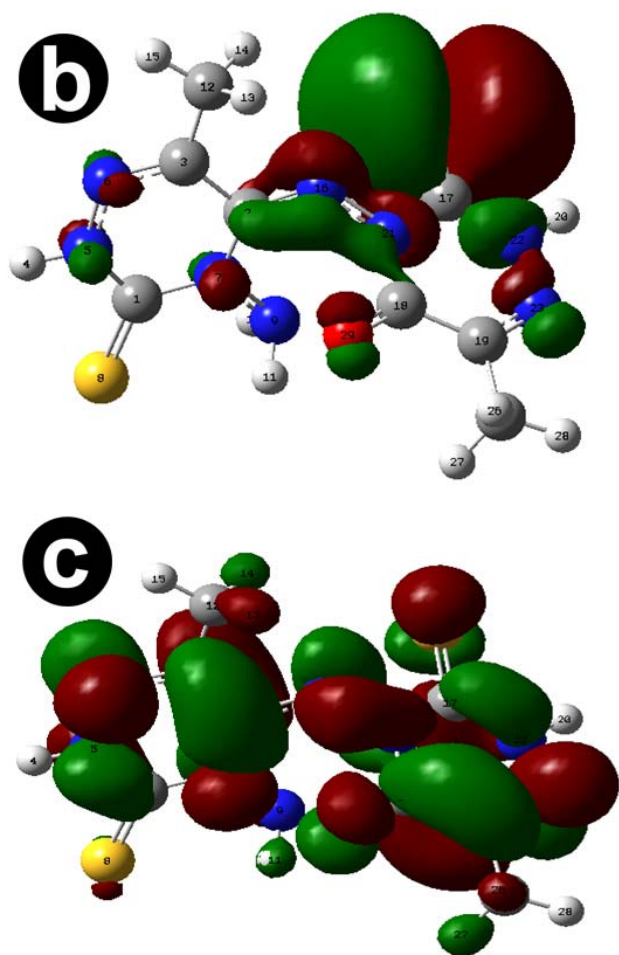


**Fig 6. (b) Highest occupied molecular orbital HOMO (c) Lowest unoccupied molecular orbital LUMO**

The condensed atom Fukui functions for electrophilic and nucleophilic attack were calculated and given in Table 5. It is clear that the most reactive electrophilic sites are S(24), C(17), N(16), and N(23) and most reactive nucleophilic sites are N(6), C(2), and N(23). Thus, it can be concluded that the data obtained from theoretical study were in agreement with that obtained from electro analytical studies.

**Table 5. Condensed atom Fukui functions for AMTDT**

Atom	$f(-)$	$f(+)$
1C	0.0002	0.0085
2C	0.0061	0.1219
3C	0.0020	0.1064
4H	0.0000	0.0001
5N	0.0054	0.0267
6N	0.0042	0.1636
7N	0.0053	0.0531
8S	0.0016	0.0063
9N	0.0002	0.0023
10H	0.0002	0.0020
11H	0.0001	0.0023
12C	0.0002	0.0015
13H	0.0002	0.0037
14H	0.0001	0.0026
15H	0.0000	0.0001
16N	0.0188	0.0830
17C	0.0444	0.0310
18C	0.0022	0.0597
19C	0.0009	0.0927
20H	0.0053	0.0001
21N	0.0094	0.0306
22N	0.0097	0.0103
23N	0.0117	0.1124
24S	0.8633	0.0314
25C	0.0008	0.0011
26H	0.0001	0.0028
27H	0.0002	0.0031
28H	0.0001	0.0000
29O	0.0071	0.0404

### SEM Analysis

The scanning electron microscopic images of the surface of copper samples were recorded in order to observe the changes that occurred during the corrosion in the absence and presence of AMTDT. The Fig.7 (a) shows the bare copper. Fig.7 (b) shows highly damaged copper specimens due to the direct attack of 0.5M HCl solution. It is clear that the surface of copper was highly corroded in the aggressive acid media. The Fig.7 (c) shows a smooth surface with the inhibitor on the surface of the copper after the addition of 200ppm inhibitor in 0.5M HCl solution. The results reveal that the protective layer formed on the surface, by means of adsorption or coordination, acts to offer excellent corrosion protection properties on 0.5M HCl solution.

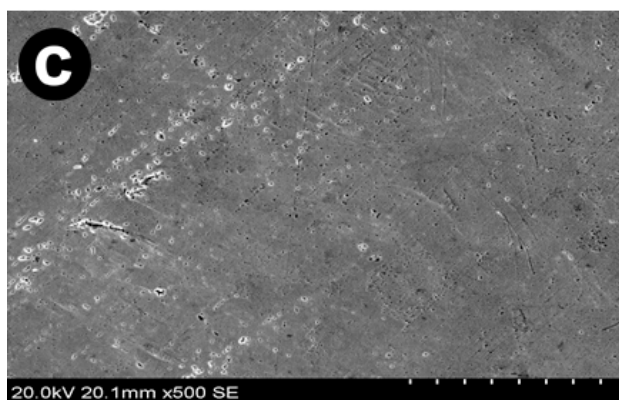
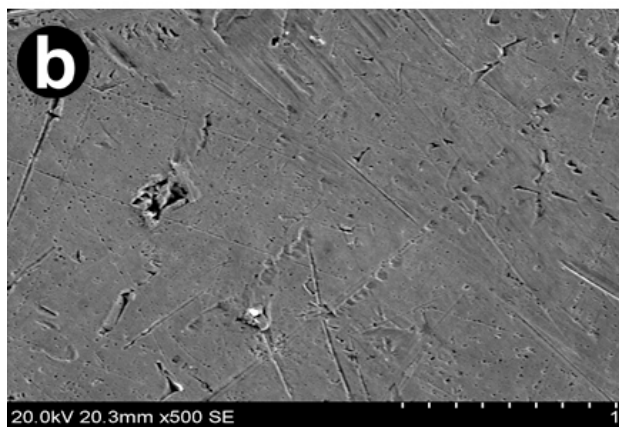
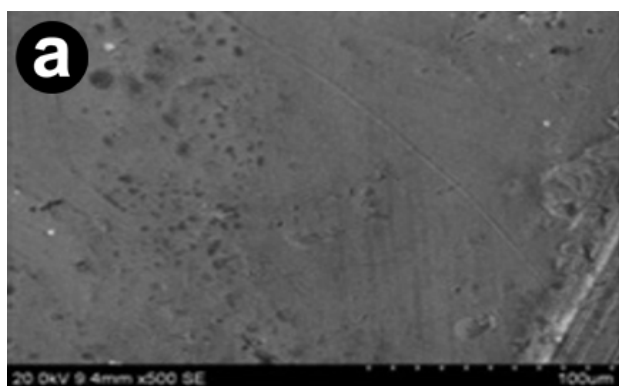


**Fig 7. SEM images (a) Bare Copper, (b) Copper in 0.5 M HCl, (c) Copper in 0.5 M HCl with AMTDT**

## CONCLUSIONS

1. The studied Schiff base AMTDT is shown to be a good inhibitor. As the concentration increases, charge transfer resistance and corrosion inhibition efficiency increases whereas the corrosion rate and double layer capacitance decreases. It is a mixed type (Cathodic/anodic) inhibitor for copper corrosion in HCl medium.

2. The inhibition process is temperature dependent, which is maximized at 313K.
3. The adsorption follows Langmuir adsorption isotherm, suggesting a multilayer formation (mixed adsorption, which is temperature dependent) on the copper surface.
4. From the SEM images, it is clear that the inhibitor molecules adsorbed on the copper surface, formed a strong protective layer in low acid concentration and weak layer in high acid concentration.
5. The computational calculations and electro analytical results confirm that the inhibitor AMTDT can act as a better inhibitor at 313K.

## REFERENCES

1. Elmersi MA, Hassanien AM. *Corros. Sci.*, 1999, 41, 2337-2352.
2. Bastidas JM, Pinilla P, Cano E, Polo JL, Mignel S. *Corros. Sci.*, 2003, 45, 427-449.
3. Tremont R, Cabrera CR. *J.Appl.Electrochem.* 2002, 32, 783-793.
4. Bentiss F, Traisnel M, Gengembre L, Lagrence M. *Appl. Surf. Sci.*, 1999, 152, 237-249.
5. Cicileo GP, Rosales BM, Varela FE, Vilche JR. *Corros. Sci.*, 1999, 41, 1359-1375.
6. Ye XR, Xin XQ, Zhu JJ, Xue ZL. *Appl. Surf. Sci.*, 1998, 153, 307-317.
7. Bragmann II in *Corrosion Inhibitors*, Macmillan, New York, 1963.
8. Behpour M, Ghoreishi SM, Salavati-Niasari M, Ebrahimi B. *Mater. Chem. Phys.*, 2008, 107, 153-157.
9. Vastag GY, Szocs E, Shaban A, Kalman E. *Pure Appl. Chem.*, 2001, 73, 1861-1869.
10. Aiad I, Ahmed SM, Dardir MM. *J. Dispers. Sci. Tech.*, 2012, 33, 317-324.
11. Yurt A, Dursun B, Dal H. *Arab. J. Chem.*, 2010, doi:10.1016
12. Li S, Chen S, Lei S, Ma H, Yu R, Liu D. *Corros. Sci.*, 1999, 41, 1273-1287.
13. Singh K, Kumar Y, Puri P, Sharma C, Aneja KR. *Med.Chem.Res.*, 2012, 21, 1708-1716.
14. John S, Joseph B, Aravindakshan KK, Joseph A. *Mater. Chem. Phys.*, 2010, 122, 374-379.
15. Chem J-L, Wu B, WuiGu, Cao X-F, Wen H-R, Hong R, Liao J, Bo-Taosu. *Trans. Met. Chem.*, 2011, 36, 379-386.
16. John S, Joseph A. *RSC Adv.*, 2012, 2, 9944-9951.
17. Darnow A, Mengel H, Marx P. *Chem. Ber.*, 1964, 97, 2173-2184.

18. ASTM G-31-72, In Annual Book of ASTM standard, ASTM International, West Conshohocken (PA), 1990, p 401.
19. El-Sayed, Sherif M. *Appl. Surf. Sci.*, 2006, 252, 8615-8623.
20. Sorkhabi HA, Shaabani B, Seitzdeh D. *Appl. Surf. Sci.*, 2005, 239, 154-164.
21. Sastri VS, Perumareddi JR. *Corrosion*, 1997, 53, 617-622.
22. Kumar SLA, Gopiraman M, Kumar MS, Sreekanth A. *Ind. Eng. Chem. Res.*, 2011, 50, 7824-7832.
23. Champion FA in *Corrosion Testing Procedure*, 2<sup>nd</sup> ed., Champion Hall, London, 1964, p 32.
24. Zhang D-Q, Gao L-X, Zhou G-D. *Appl. Surf. Sci.*, 2004, 225, 287-2903.
25. Ohsawa M, Suetaka W. *Corros.Sci.*, 1979, 19, 709-722.
26. Samide A, Tutunaru B. *Part A: Toxic/Hazardous Substances and Environmental Engineering*, 2011, 46, 1713- 1720.
27. Yan Y, Li W, Cai L, Hou B. *Electrochem. Acta*, 2008, 53, 5953-5960.
28. Li W, Zhao X, Liu F, Deng J, Hou B. *Corros.*, 2009, 60, 287-293.
29. Morad MS. *J. Appl. Electrochem.*, 2007, 37, 1191-1200.
30. Abdullah M. *Corros. Sci.*, 2002, 44, 717-728.
31. John S, Mohammed Ali K, Joseph A. *Bull. Mater. Sci.*, 2011, 34, 1245-1256.
32. Fouda AS, Elewady GY, Abdel-Fattah AM. *Protection of Metals and Physical Chemistry of Surfaces*, 2011, 47, 253-263.
33. Eddy NO. *Molecular Simulation*, 2010, 36, 354-363.
34. Tang Y-M, Yang W-Z, Yin X-S, Liu Y, Wan R, Wang J-T. *Mater. Chem. Phys.*, 2009, 116, 479-483.
35. Amin MA, Khaled KF, Fadi SA. *Corros. Sci.*, 2010, 52, 140-151.
36. Venkata R, Gorantla, Matijevic E, Babu SV. *Chem.Mater.*, 2005, 17, 2076-2080.